JOURNAL OF GEOPHYSICAL RESEARCH, VOL. 86, NO. A1, PAGES 37-53, JANUARY 1, 1981

A GROUND-SATELLITE STUDY OF WAVE-PARTICLE CORRELATIONS

C. G. Park

Radioscience Laboratory, Stanford University, Stanford, California 94305

C. S. Lin[1]

Space Sciences Division, Geophysics Program, University of Washington, Seattle, Washington 98195

G. K. Parks

Space Sciences Division, Geophysics Program, University of Washington, Seattle, Washington 98195
Departments of Atmospheric Sciences and Physics, University of Washington, Seattle, Washington 98195

Abstract. Very low frequency (VLF) waves recorded at Siple, Antarctica (L ~ 4; 84°W, geographic), are compared with low-energy (<50 keV) electron data from the geostationary satellite ATS 6. During the period of this study (August 10-21, 1974) the satellite was anchored at 6.6 R_E and 106.5°W, near the outer edge of the nominal 'viewing area' of the Siple VLF receiver, which is estimated to be L ~ 2-6 and ±20° longitude. The results reveal two distinct types of chorus observed at Siple. One type is closely correlated with enhanced fluxes of >5-keV electrons detected at the synchronous altitude, and its generation region is inferred to be outside the plasmapause. The chorus upper cutoff frequency increases with time in a characteristic manner, consistent with the expected adiabatic motion of injected electrons in cyclotron resonance with the waves. The second type of chorus, which we refer to as 'plasmaspheric chorus,' occurs inside the plasmapause, has no apparent relationship to particle injection at the synchronous altitude and shows clear evidence of being triggered by whistlers, power line radiation, and other signals. The two different types of chorus are readily distinguishable in frequency-time spectrograms.

1. Introduction

A widely accepted theory of whistler mode VLF wave generation in the magnetosphere involves cyclotron resonance interaction with energetic electrons [e.g., Kennel and Petschek, 1966; Dysthe, 1971; Nunn, 1974; Helliwell and Crystal, 1973]. Wave growth by this mechanism depends on the resonant electron flux as well as on the pitch angle distribution. Anderson [1976] and Anderson and Maeda [1977] found close correlation between VLF emissions and enhanced fluxes of anisotropic electrons detected on the Explorer 45 satellite, corroborating the cyclotron resonance theory. Statistical studies of VLF chorus [Tsurutani and Smith, 1974; Thorne et al., 1977; Park and Miller, 1979] as well as case studies [Carpenter et al., 1975; Foster et al., 1976; Tsurutani et al., 1979] showed that chorus is correlated with magnetospheric substorm activity, indicating that freshly injected particles play a central role in wave generation. On the other hand, there is evidence that waves entering the magnetosphere from below, such as whistlers, power line radiation (PLR), and VLF transmitter signals can trigger emissions under conditions not conducive to spontaneous emission generation [Storey, 1953; Helliwell, 1965; Helliwell and Katsufrakis, 1974; Helliwell et al., 1975]. A statistical study of ground-based VLF data also indicated that triggering is an important factor [Park and Miller, 1979].

In this paper, VLF wave data from Siple, Antarctica (76°S, 84°W; L ≃ 4), and simultaneous particle data from the ATS 6 satellite are used to study wave-particle correlations in an attempt to clarify the role of particles in the generation of VLF waves. Magnetospheric VLF waves that penetrate the ionosphere tend to spread over large areas in the earth-ionosphere waveguide, and the nominal 'viewing area' of the Siple receiver is estimated to be L ~ 2-6 and ±20° longitude [e.g., Carpenter, 1970]. The present study covers 12 consecutive days, August 10-21, 1974, during which simultaneous wave and particle data were available. During the 12-day period, ATS 6 was anchored at 6.6 R_E and 106.5°W longitude, near the outer edge of the L-longitude space that can be monitored by the VLF receiver at Siple. Observations from two geostationary platforms have permitted detailed studies of the temporal development of wave and particle behavior on a continuous basis.

The wave and particle data show two distinct classes of chorus events. One class involves particle injection associated with magnetospheric substorms and can be inferred to occur outside the plasmapause. The other class of chorus events shows no apparent relationship to particle injection but shows clear evidence of triggering by whistlers, PLR, and other emissions inside the plasmapause.

2. Sources of Data

The Siple VLF data used in this study were acquired using a calibrated receiver with a 435-m^2 loop antenna (see Helliwell and Katsufrakis [1978] for further details). The broadband output of the receiver was recorded on magnetic tapes on a synoptic schedule of 1 min every 5 or 15 min. In addition, the receiver output was fed into a 2-to-4-kHz bandpass filter and a dual

[1]Now on leave at the Institute for Physical Science and Technology, University of Maryland, College Park, Maryland 20742.

Paper number 80A0876.
0148-0227/81/080A-0876$1.00

time constant detector with a rise time of ~1 s and a fall time of ~0.1 s. This detector was designed to discriminate against sferics, individual whistlers, and other isolated, impulsive signals. The detector output was then recorded continuously on a chart recorder.

The particle data come from two different instruments on ATS 6. The University of Minnesota instrument provided electron flux data in the energy range of ~32-44 keV with equatorial pitch angles of ~90°. Details of this instrument have been described by Walker et al. [1975]. The University of California, San Diego (UCSD), plasma experiment provided phase-space densities and pitch angle distributions of electrons in the ~0.1- to 81-keV range. The data used in this study come from the north-south detector mounted on a mechanical platform that could scan the pitch angle range of a few degrees to ~140° in ~120 s. Further details of the instrument characteristics are given by Mauk and McIlwain [1975].

3. An Overview

Figure 1 shows plots of Siple VLF wave amplitude (2-4 kHz), ATS 6 electron flux (32-44 keV, $\alpha \simeq 90°$, from the University of Minnesota detector), and the auroral electrojet (AE) index during the period August 10-21, 1974. The VLF data shown here are 1-min averages taken every 15 min from continuous chart recording. (Samples of original chart recording will be shown later.) Wave, particle, and AE activities all tend to come in bursts that stand out clearly above the background quiescent level. Large increases in trapped particle flux are a feature commonly observed in association with substorms at synchronous altitudes [Lezniak and Winckler, 1970; Parks, 1970]. Slow decreases in flux just prior to substorm injection (for example, between 0400 and 0500 UT on August 10, 1974) are due to the inward convection of trapped particle drift shells and are a characteristic feature of substorm injection events in the premidnight sector [Lin and Parks, 1974; Bogott and Mozer, 1973; Lezniak and Winckler, 1970]. Gaps between 1700 and 2200 UT are due to the absence of good particle data during that time interval.

VLF waves may have a variety of spectral characters depending on their origin. Descriptive letters in Figure 1 identify the dominant types of waves contributing to the VLF events, as determined from broadband spectral data: chorus (c), hiss (h), whistlers (w), and power line radiation (p). The AE indices come from the 11-station analysis published by the World Data Center A.

Figure 1 shows clearly correlated wave and particle events that are also accompanied by enhancements in AE index. Such correlated events are indicated by vertical lines at the time of event onset on August 10, 11, 13, 16, 17, 18, and 19. After about 0800 UT on August 19 there is continuous substorm activity through August 21, and it is difficult to make event-by-event association between VLF, electron flux, and AE data. Between August 10 and 19 we see that all clear cases of electron flux enhancements above $\sim 5 \times 10^5$ el cm^{-2} s^{-1} keV^{-1} and lasting for half an hour or more are accompanied by enhanced VLF activity. Chorus is the predominant wave form during these events, although some hiss, echoing whistlers, and power line radiation are also observed.

There are also significant enhancements in VLF intensity that are not accompanied by enhancements in electron flux or AE index. Some of these VLF enhancements involve only whistlers and hiss but not chorus; examples are found on August 12 and 18. Hiss in these cases is band limited (~2-5 kHz) and originates in long-enduring whistler echo trains [see Helliwell, 1965]. This type of hiss is distinct from auroral hiss (above ~4 kHz), generally observed at higher latitudes, and plasmaspheric ELF hiss (~0.5-3 kHz) [e.g., Thorne et al., 1973; Muzzio and Angerami, 1972]. The events involving only whistlers and their echoes will not be discussed further in this paper.

Some chorus activity is also observed without accompanying increases in equatorial electron fluxes. Examples include the events starting near 1000 UT on August 14 and near 0500 UT on August 15. The chorus spectra during these events will be examined in detail in section 5. It will then be shown that there are fundamental differences in spectral characteristics between chorus activity occurring with and without accompanying particle injection detected by ATS 6.

In several cases wave and particle events appear to be related, but their relationship cannot be established with certainty. The PLR and chorus activity near 1200 UT on August 15 and the chorus activity near 1100 UT on August 17 belong to this category. These cases will be examined in detail in section 5. On August 14, particle data were contaminated by sunlight during the event starting near 1700 UT. However, the small increase in AE at 1500 UT suggests that there may have been a low-level particle injection. This question cannot be resolved with the available data. A similar difficulty is found near 2000 UT on August 17.

In summary, strong particle injection events at ATS 6 are accompanied by chorus and other wave activity at Siple; however, not all chorus events are accompanied by particle injection at ATS 6. Sections 4 and 5 will examine the details of particle and wave data during correlated wave-particle events as well as the nature of chorus events that are not accompanied by particle events.

4. Details of Correlated Events

During three correlated wave-particle events the UCSD instrument was in a mode of operation that provided information on the phase space distribution function as well as the usual pitch angle distributions. Electrons of ~1- to 50-keV energies underwent significant changes during the injection events shown in Figure 1. The details of wave and particle data during each event are described below.

August 10, 1974. Figure 2 shows a continuous record of VLF intensity in the 2- to 4-kHz band (top) and frequency-time spectrograms taken for approximately 1 min every 5 min (bottom). The time marks at the bottom of the lower panel indicate the beginning of each 1-min sample.

The first sign of chorus appears in the 0505 UT record below 1.7 kHz. The upper cutoff frequency increases with time to about 2.8 kHz at 0520 UT. On the basis of the spectrogram we can place the chorus onset time between 0501 and 0505

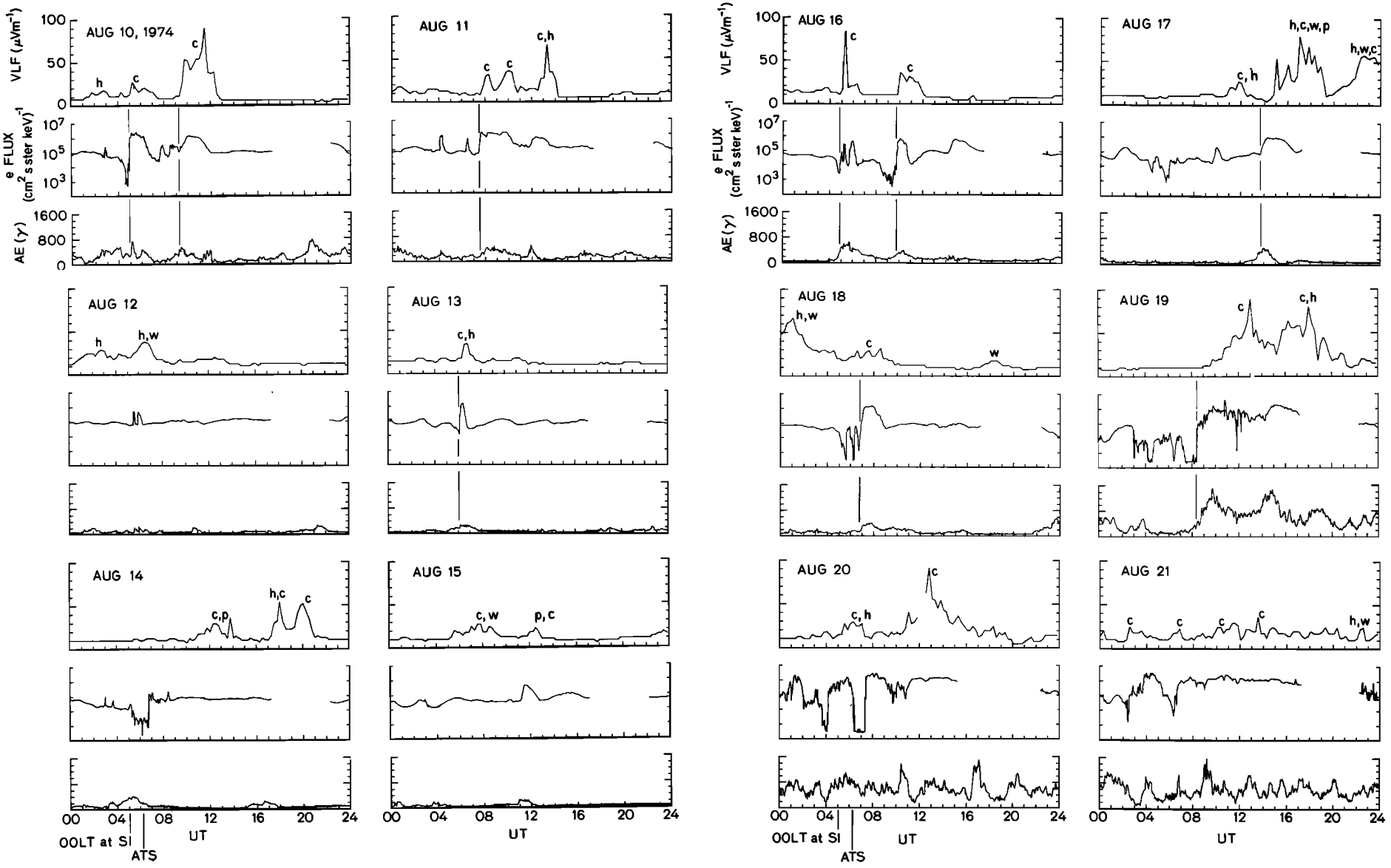

Fig. 1. Plots of VLF activity in the 2- to 4-kHz band recorded at Siple, Antarctica, energetic electron flux in the ~32- to 44-keV energy range detected at the ATS 6 satellite, and auroral electrojet index for the period August 10-21, 1974. The vertical lines indicate the onset of correlated wave-particle events. Descriptive letters, c for chorus, h for hiss, w for whistlers, and p for power line radiation, indicate the dominant wave types composing each VLF event.

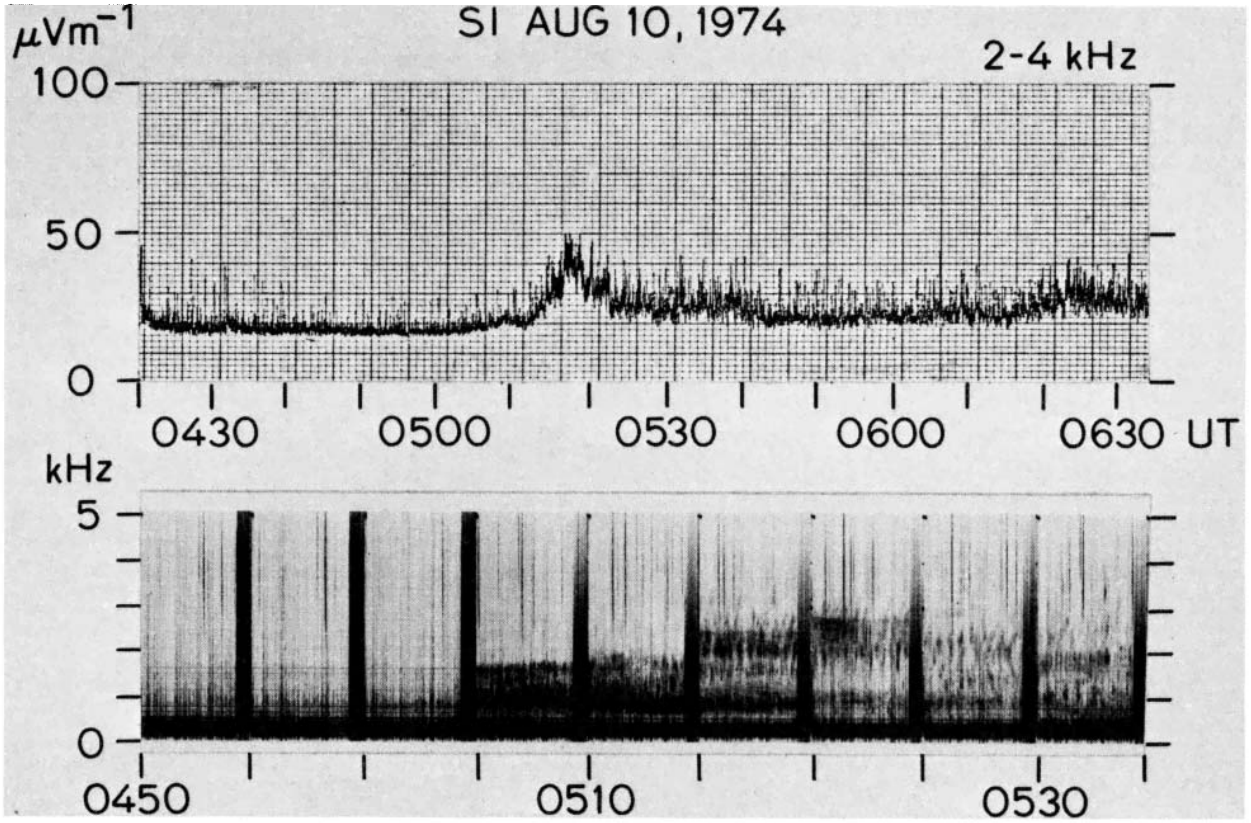

Fig. 2. VLF wave amplitude (top) and broadband spectrograms (bottom) recorded at Siple, Antarctica. The tick marks at the bottom indicate the beginning of ~1-min samples taken every 5 min.

UT. (Note, however, that the 2-to-4-kHz intensity record does not show noticeable enhancement until about 0512 UT, when the chorus upper cutoff frequency apparently reached the lower edge of the passband.)

Figures 3 and 4 show the particle data from the UCSD detector during this event. The data were fitted to form $F = F_0 \sin^m \alpha$ at selected energy levels. The behavior of the distribution function is clearly energy-dependent (Figure 3). At low energies (for example, 5.4 keV) the signature of injection onset is evident, but the distribution function does not change significantly. Above 21 keV, however, the distribution function increases sharply, up to 2 orders of magnitude. This increase nearly coincides with VLF onset. Further discussion of the behavior of different energy particles during substorms is given by Parks et al. [1977].

Figure 4 shows the behavior of the pitch angle distribution for three energies as a function of time. Note the presence of strongly field-aligned components (negative m) first at 47.4 keV and then at 1.4 keV a few minutes later. The 47.4-keV electrons subsequently changed to a strong loss cone distribution ($m \simeq 1$) before returning to the preinjection shape. The 1.4-keV electrons returned to nearly isotropic distribution ($m \simeq 0$) following injection. Another way to illustrate the pitch angle behavior is to plot the actual pitch angle distribution. Figure 5 shows an example taken just after the injection. The field-aligned 1.4-keV electron fluxes and the peaked large pitch angles of the higher-energy particles corroborate the features indicated for the time interval ~0505-0508 UT in Figure 4.

August 16, 1974. Figure 6 shows the wave data for this case in the same format as Figure 2. In this case, however, broadband synoptic recording

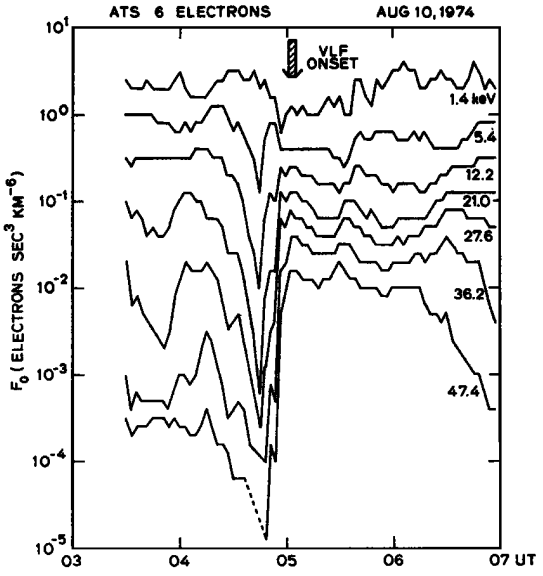

Fig. 3. Electron flux versus time at several energies for the VLF event of Figure 2.

was made for 1 min every 15 min. The upper cutoff frequency of chorus was ~2 kHz when the chorus first appeared at 0505 UT, but it increased to ~3 kHz at 0520 UT. At 0605 and 0620 UT the spectrogram shows horizontal striations near 2 kHz. The amplitude record shows the first sign of enhancement at 0503 UT. Combining the amplitude and spectral data, we determine that the chorus onset occurred between 0451 and 0503 UT.

To show selected portions of the spectra in greater detail, 0520 and 0605 UT records have been expanded and reproduced in Figure 7. The 0520 UT data that look like hiss in the time-compressed record of Figure 6 now appear as chorus with closely spaced discrete elements. The horizontal lines in the lower panel are similar to amplified power line harmonic radiation reported previously [Helliwell et al., 1975; Park, 1977].

The particle data for this case are shown in Figure 8. The UCSD particle detector was in a nonscanning mode, and therefore the pitch angle coverage during the time interval shown was limited to 43°-58°. Large phase-space density changes are evident at the time of VLF onset for energies above 5.4 keV. The general behavior of the particle distribution function is similar to that of the August 10 case, although there are differences in details. For example, on August 16 multiple injections are apparent for electrons with ≳21-keV energy.

August 18, 1974. This case is illustrated in Figures 9-11. From the spectrogram in Figure 9 the VLF onset is estimated to have occurred between 0651 and 0705 UT. We note once again that the upper cutoff frequency increased systematically with time following onset. The 2- to 4-kHz intensity record shows many sharp spikes before 0700 UT that are due to strong whistlers and their echoes. These echoing whistlers appear as almost vertical but slightly curved lines in the spectrogram.

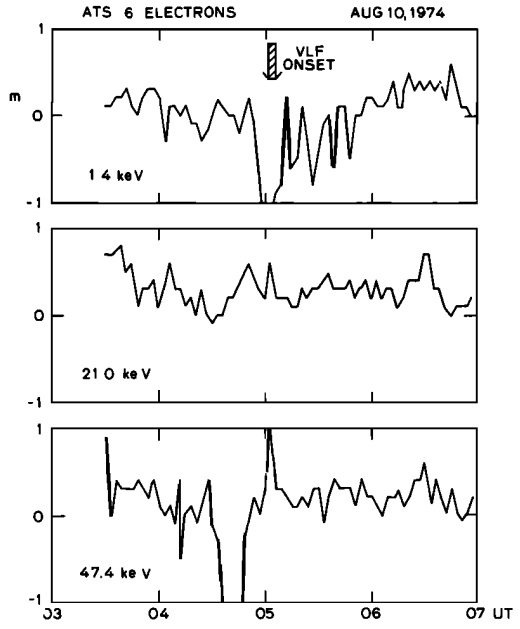

Fig. 4. Electron pitch angle anisotropy parameter versus time at three energies for the period covered in Figure 3. Typical error is ~0.1 or less.

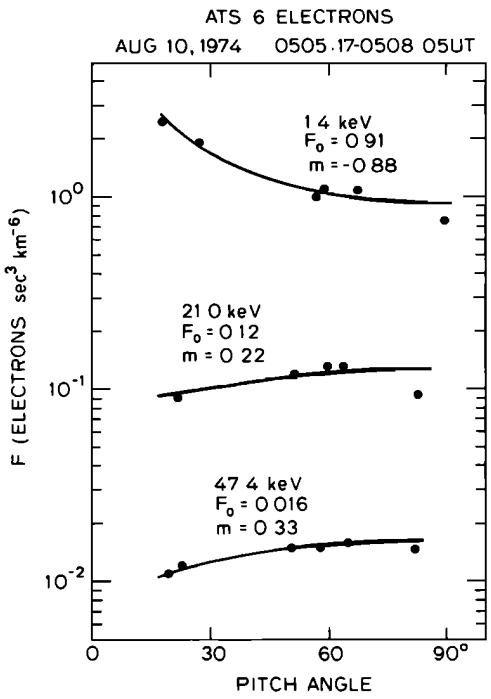

Fig. 5. Electron pitch angle distribution at three energies immediately after the injection event in Figure 3.

Figure 10 illustrates the particle behavior in this case. There were several particle injections between 0500 and 0800 UT. The injection that occurred at ~0658 UT is correlated with the VLF wave activity. The main difference between this injection and the earlier injections is in the intensity of ≳21-keV electrons. Fluxes for the 0658 UT injection were significantly larger [see Parks et al., 1977]. Figure 11 shows the behavior of the pitch angle distribution. Note, as before, the presence of field-aligned components prior to each injection (indicated by $m < 0$). For >10-keV electrons, m becomes positive after each injection, but in terms of the pitch angle distribution the 0658 UT injection was not markedly different from earlier injections.

Summary and discussion of correlated events. In the three cases discussed above, chorus activity started at Siple within 10-15 min of particle injection observed at ATS 6. Siple was within ~0000-0200 MLT at the time of chorus onset. A characteristic feature of chorus activity accompanied by particle injection is that the upper cutoff frequency f_{uc} increases systematically with time following onset. Positive df_{uc}/dt, similar to the three cases illustrated above, is clearly observed in all but one set of correlated events marked by vertical lines in Figure 1. The only exception is the event near 1000 UT on August 16. In this case, chorus first appeared in the 1005 UT record with f_{uc} = 2.5 kHz and did not show a systematic increase with time. To understand this unusual behavior, simultaneous VLF spectral data from Halley Bay, Antarctica (L ~ 4 and 2 hours MLT east of Siple), were examined. It was found that at Halley Bay, chorus

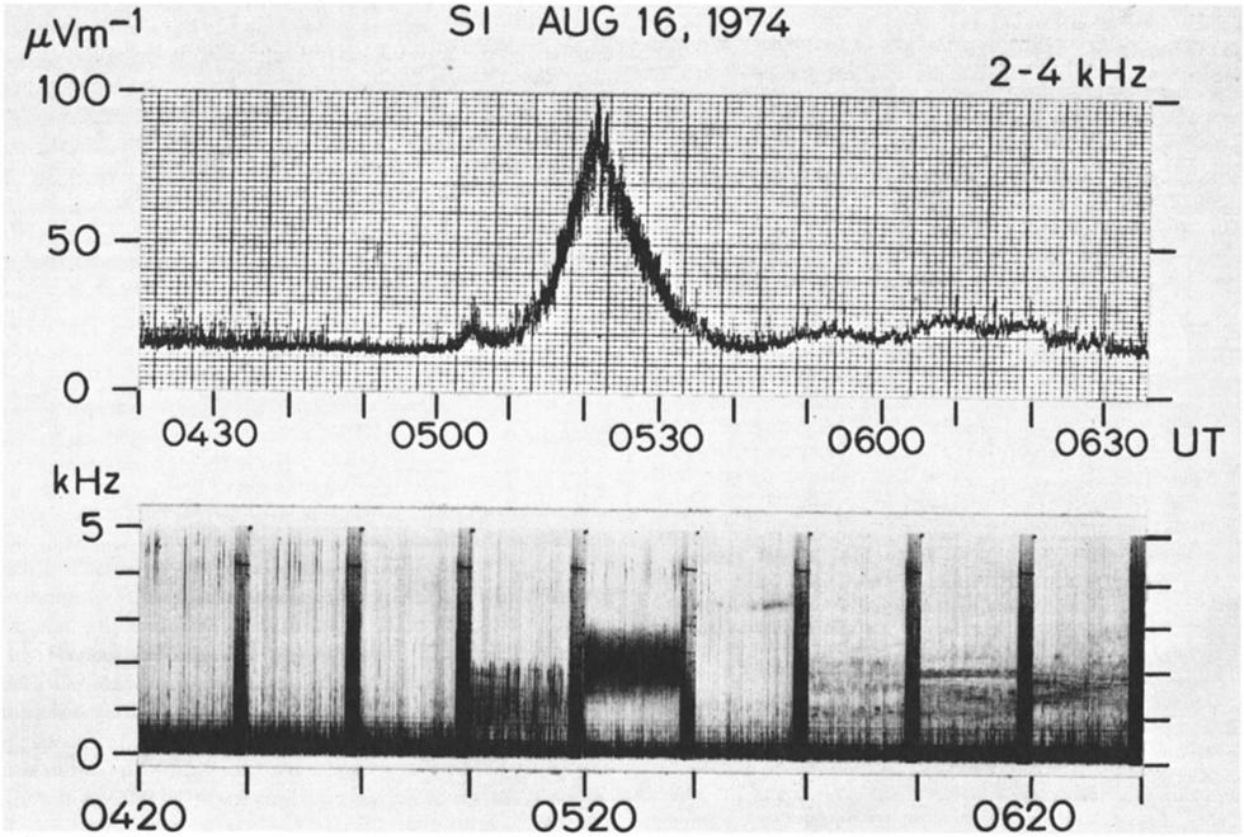

Fig. 6. VLF wave amplitude (top) and broadband spectrograms (bottom) recorded at Siple, Antarctica. The tick marks at the bottom indicate the beginning of ~1-min samples taken every 15 min.

started at 1005 UT and f_{uc} increased with time for about 1 hour in the manner illustrated in Figures 2, 6, and 9. Why Siple did not record similar behavior is not clear, but it is possible that the rising portion of the chorus was not recorded there because no duct was present.

Two possible explanations have been discussed in the literature for the tendency of f_{uc} to increase with time [Carpenter et al., 1975; Foster et al., 1976; Park, 1977; Thomas, 1979]. One possible explanation is that when energetic particles are injected earthward from the nightside magnetosphere, the electric field that injects energetic particles imparts the same $\vec{E} \times \vec{B}$ drift velocity to the thermal plasma. Since there is a tendency for chorus frequency to track the equatorial electron gyrofrequency [Burtis and Helliwell, 1976], chorus generated inside an inward drifting duct would increase in frequency. Another possible explanation involves the longitudinal drift of injected energetic electrons. If energetic electrons are injected near midnight and if a duct that guides chorus to a ground station is somewhere to the east of the injection zone, then the energetic electrons reach the duct through gradient and curvature drift. Since this drift is energy-dependent, higher-energy electrons arrive first, followed by electrons of progressively lower energy. The condition for cyclotron resonance, which is generally believed to be the generation mechanism for chorus, is given by

$$f = \frac{f_H}{1 + v_{\parallel}/v_p} \qquad (1)$$

where f_H is the electron gyrofrequency, f is the wave frequency, $v_{\parallel}$ is the parallel electron velocity, and v_p is the wave phase velocity. It can be shown that for $f < f_H$, which is a necessary condition for whistler mode waves, $df/dv_{\parallel}$ is always negative. Thus lower-energy particles arriving later generate higher-frequency waves. Thomas [1979] examined the two mechanisms quantitatively and came to the conclusion that both mechanisms are needed to explain observations. Inward drift of chorus-generating ducts is more important before 0400 MLT, whereas energy-dependent dispersion of the electron cloud is more important after 0400 MLT.

The one important parameter in the particle data at the time of the chorus onset is the large increase in electron fluxes above some critical energy level that varies from ~5 to ~25 keV. Pitch angle anisotropy, although highly variable and of the 'loss cone' shape at injection, shows about the same average value before and after the chorus onset. The anisotropy is generally positive (for energies where the flux shows significant enhancements) and satisifes one necessary condition for the cyclotron instability [Kennel and Petschek, 1966]. However, the growth rate also depends on the resonant electron flux, and the data show that the flux is a key parameter

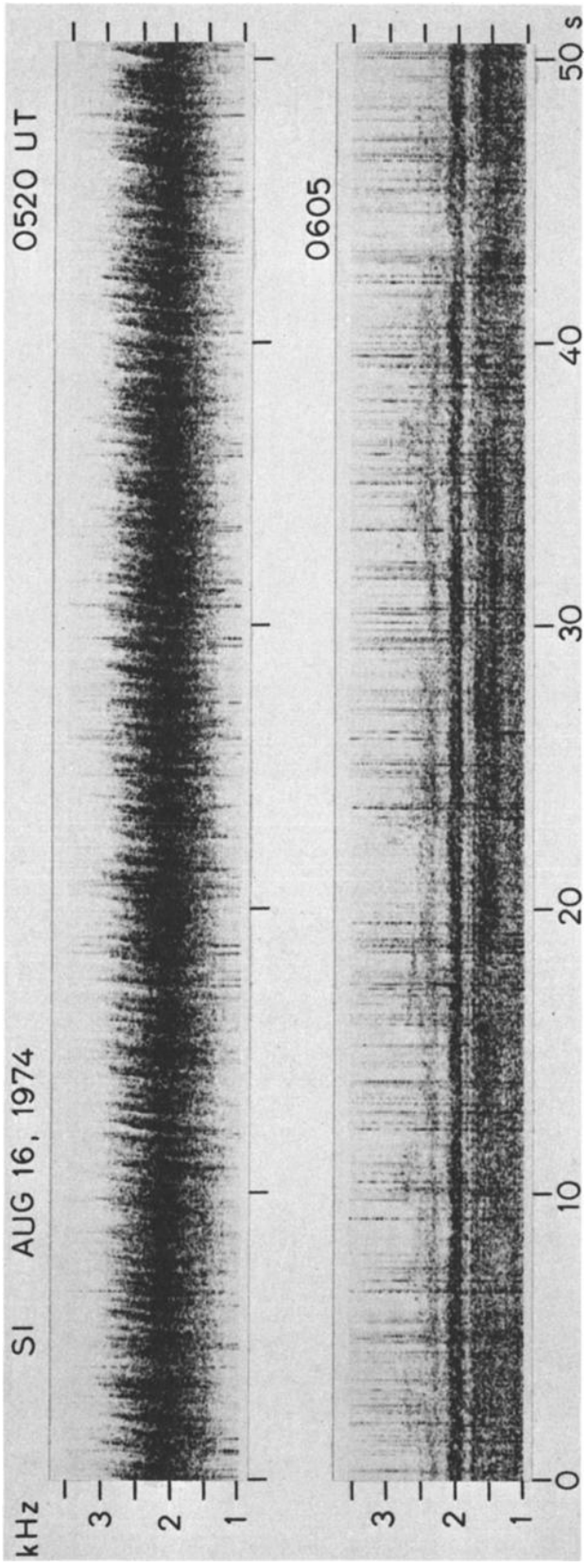

Fig. 7. Selected spectrograms in Figure 6 reproduced on expanded scales.

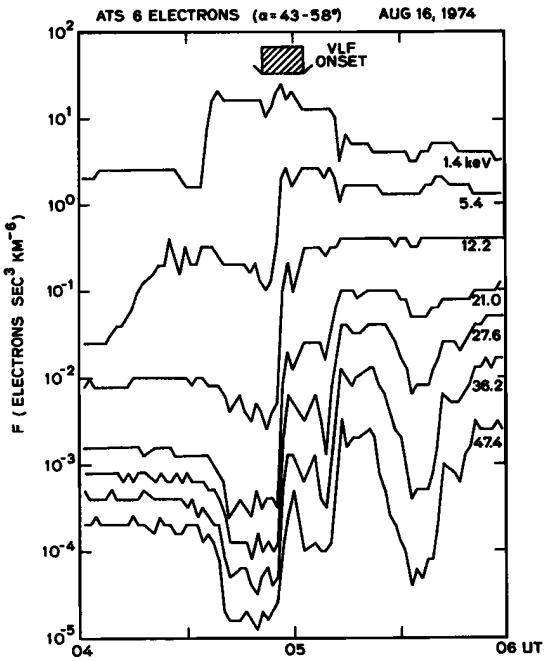

Fig. 8. Electron flux versus time at selected energies for the event illustrated in Figure 6.

in chorus generation (see Kaye et al. [1978] for a discussion of observed pitch angle anisotropy and the cyclotron precipitation theory).

The VLF receiver at Siple has a fairly large 'collecting area' (L ~ 2-6, ±20° longitude). Thus is it not possible to pinpoint the chorus generation region. However, certain inferences can be drawn from consideration of resonance and propagation conditions. For propagation along the static magnetic field the wave phase velocity can be closely approximated by

$$v_p = c \frac{f^{1/2}(f_H - f)^{1/2}}{f_p} \qquad (2)$$

where f_p is the plasma frequency. Combining this equation with (1), we obtain

$$v_\parallel = \frac{c}{f_p} \frac{(f_H - f)^{3/2}}{f^{1/2}} \qquad (3)$$

Figure 12 shows the variation of the parallel resonant energy $W_\parallel = \frac{1}{2}mv_\parallel^2$ as a function of L in a dipole geomagnetic field for f = 3 kHz. The thermal plasma density is assumed to be 6 el cm^{-3} at L = 4 and varying as L^{-4}, a model appropriate for the region outside the plasmapause [e.g., Park et al., 1978]. Since 3 kHz is approximately the maximum chorus frequency observed in each of the three cases discussed above, the resonant $W_\parallel$ must lie above the curve in Figure 12.

If we assume that chorus is generated at the equator, ducting is possible up to one half of the equatorial gyrofrequency. The maximum chorus frequency of 3 kHz places an upper limit on the L value of the generation region at L = 5.25, as indicated by a verticle line in Figure 12. (This rough estimate is based on a dipole geomagnetic

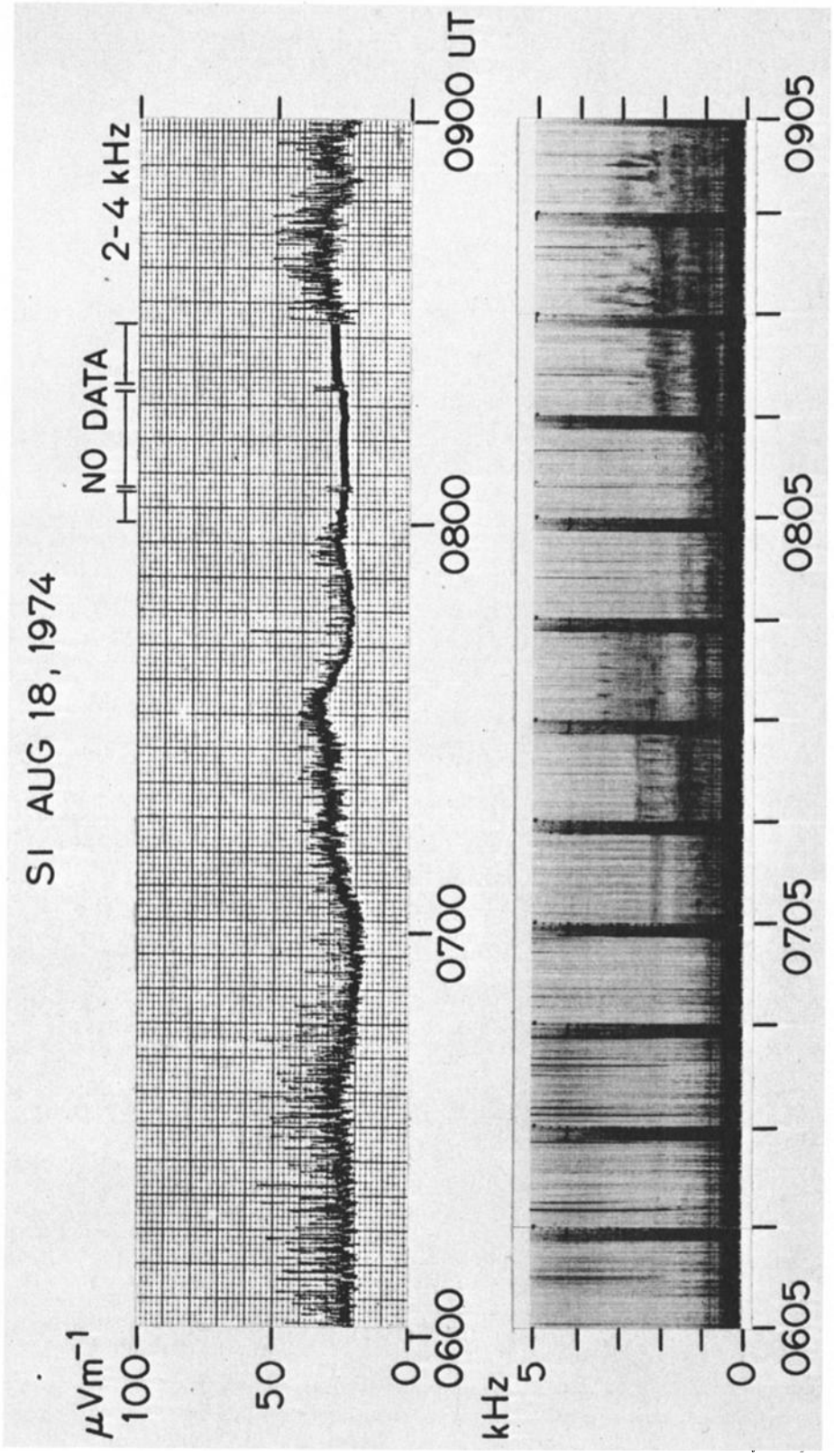

Fig. 9. VLF wave amplitude (top) and broadband spectrograms (bottom) recorded at Siple, Antarctica. The tick marks at the bottom indicate the beginning of ~1-min samples taken every 15 min.

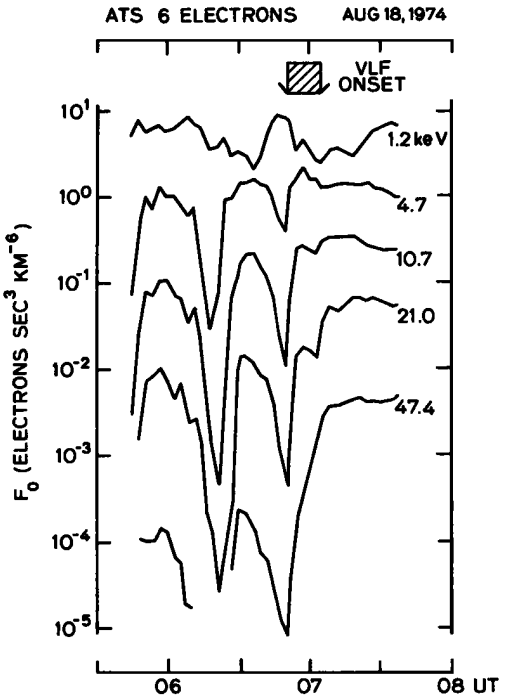

Fig. 10. Electron flux versus time at selected energies for the event illustrated in Figure 9.

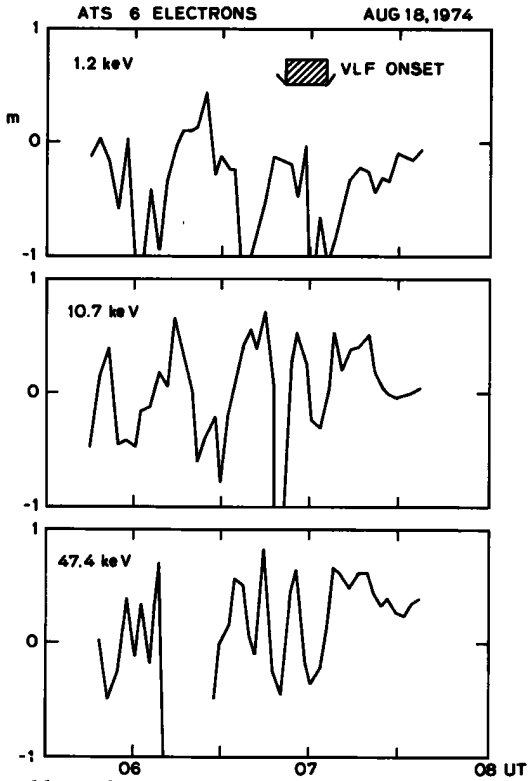

Fig. 11. Electron pitch angle anisotropy parameter versus time at three energies for the period covered in Figure 10.

field. If the equatorial field strength is depressed by 50 γ [e.g., Cummings and Coleman, 1968], the vertical line would be displaced inward by ~0.5 L.) Thus a generation region near the equator, L ≈ 5-5.25, and outside the plasmapause would be consistent with both wave and particle data. If the generation region were inside the plasmapause, then the thermal plasma density would increase by a factor of about 50, and the resonant $W_{\parallel}$ would decrease by the same factor. Since the particle data during substorm injection do not show flux increases at such low energies, we can conclude that the generation region was outside the plasmapause if freshly injected particles were responsible for the observed chorus bursts. It is possible that the chorus was generated by some preexisting plasma clouds drifting in longitude inside L = 6.6. However, this is not a likely explanation for the type of chorus discussed here, because there is no reason why the arrival of drifting clouds at a given longitude should correlate with substorms. On the other hand, preexisting plasma clouds may play an important role in the generation of the second type of chorus discussed in section 5.

5. Details of Uncorrelated Events

In this section we examine the wave characteristics during VLF events that are not associated with particle injection at ATS 6. The results will show several important features that clearly distinguish these events from the particle-associated events discussed in section 4.

August 14, 1974. Figure 13 shows spectrograms of the chorus event that started at ~1010 UT. The top panel shows ~1-min samples every 5 min. Chorus frequency was ~2-3 kHz at the onset and remained unchanged, in sharp contrast to the systematically increasing trend found in the particle-associated events. The bottom panel shows the 1015 UT record in expanded scale; many emissions are preceded by short horizontal lines, which suggest the possibility of triggering.

A short time later, evidence of triggering becomes clearer, as is illustrated in Figure 14. Chorus dominates the spectrum above ~2.8 kHz, while hiss dominates at lower frequencies. A close examination of chorus elements shows the

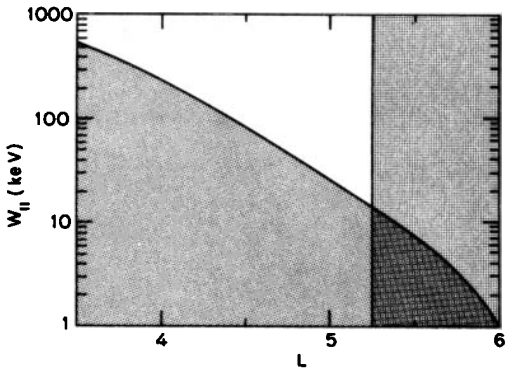

Fig. 12. Equatorial parallel energy of cyclotron resonant electrons as a function of L value assuming a dipole field and thermal plasma densities appropriate for outside the plasmapause. For plasmaspheric density fields the curve would be lowered by a factor of ~50. See text for details.

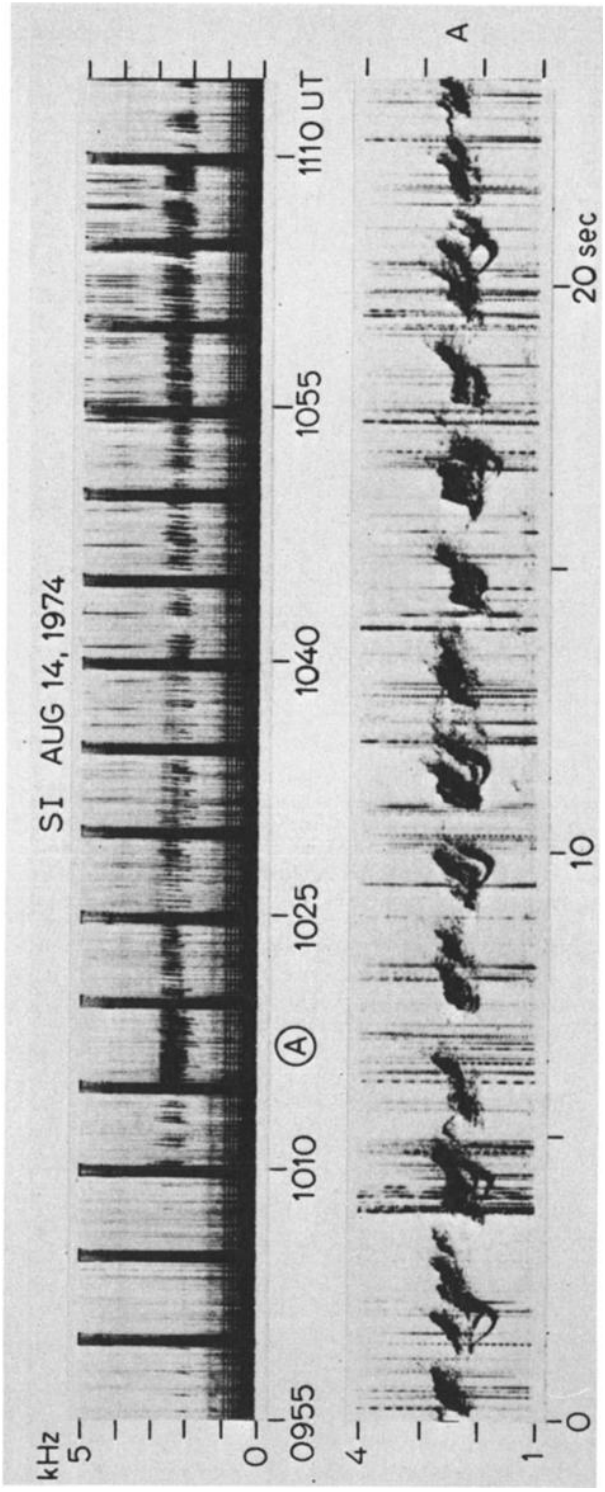

Fig. 13. The top panel shows a seris of ~1-min sample spectrograms taken every 5 min. The lower panels show the 1015 UT sample in expanded scale.

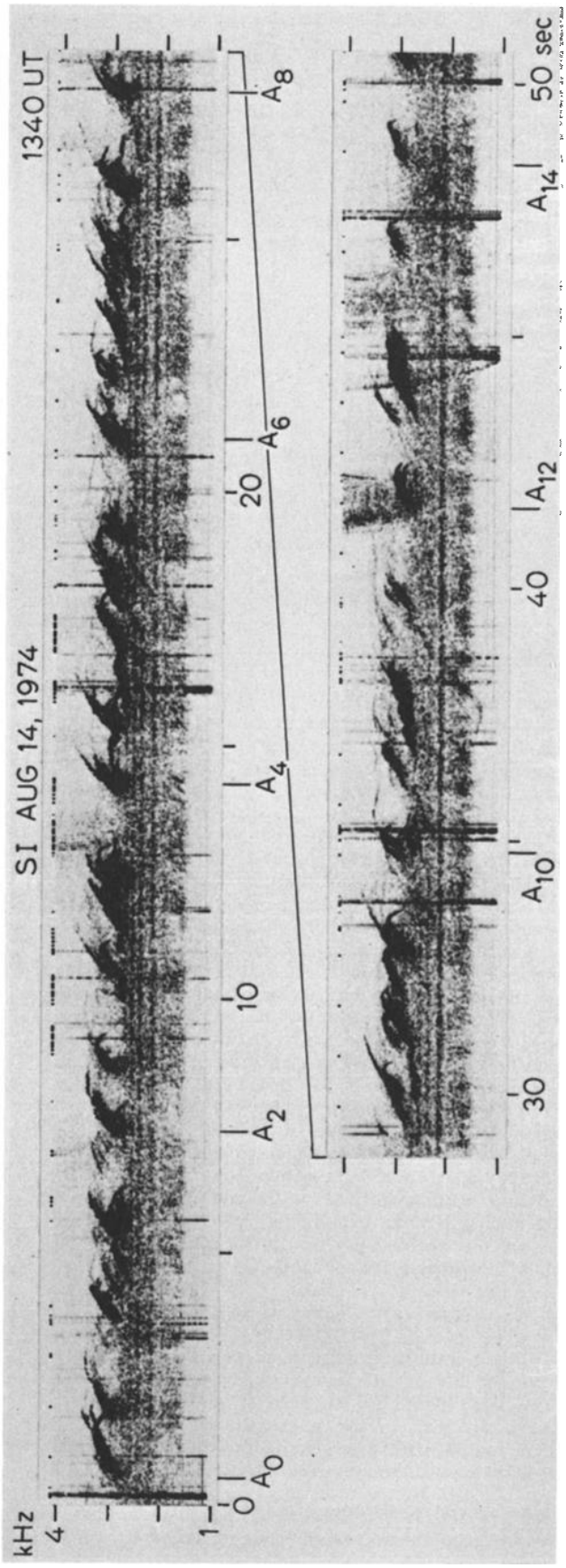

Fig. 14. Spectrograms illustrating details of chorus and hiss.

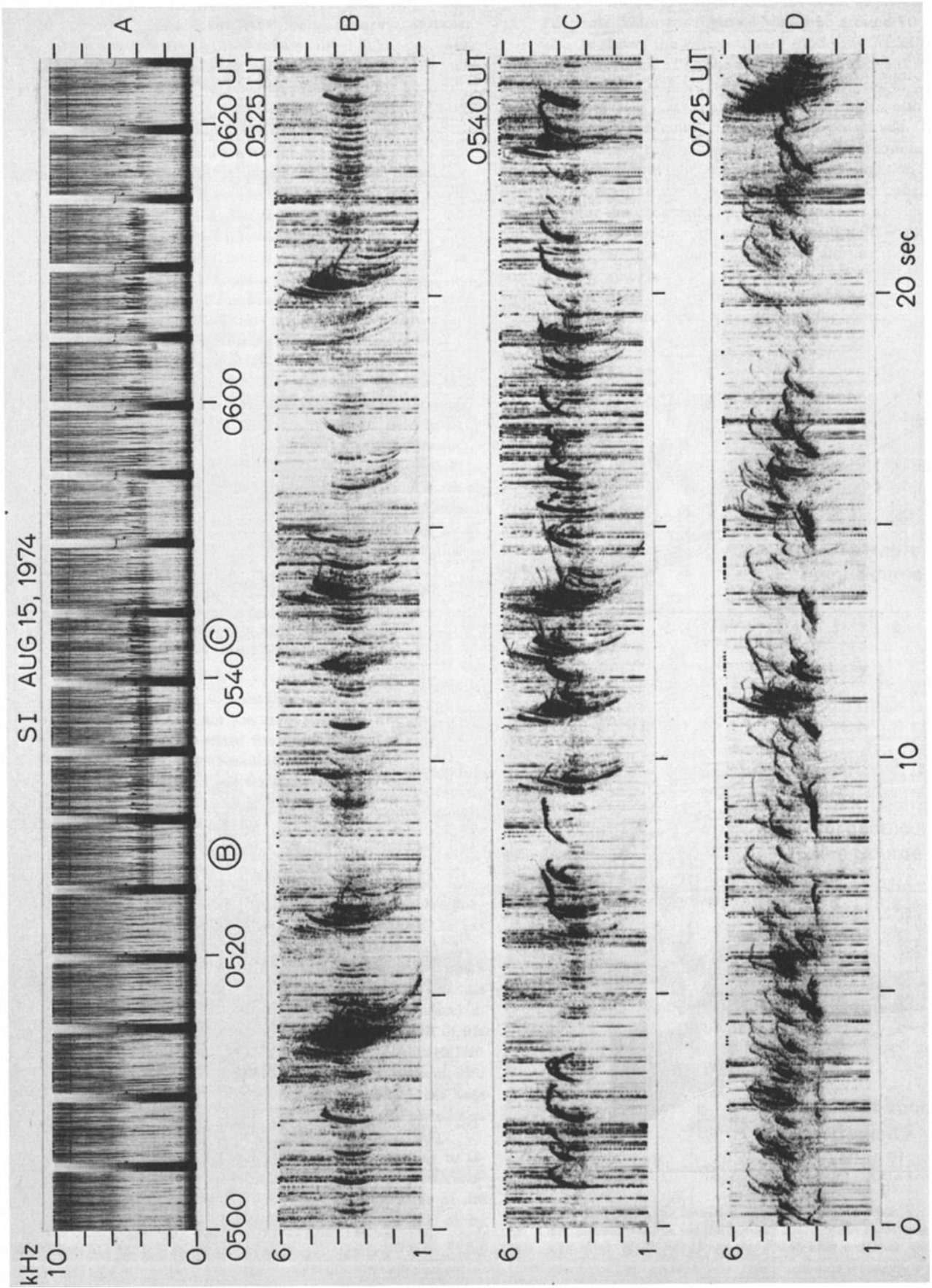

Fig. 15. The top panel shows a series of ~1-min sample spectrograms taken every 5 min. The three lower panels are expanded versions of selected samples.

basic pattern of emissions in the first 6 s of the record repeating many times. The first element in each group is labeled A_0 to A_{14}. From the spectral shape of these emissions it is clear that they are not simply successive echoes of the same wave packet. If this were the case, each successive echo would become more dispersed in a systematic way. Instead the observed emissions suggest that they are new emissions triggered each time by the echo of the previous emission. Such emissions belong to the category of nondispersive periodic emissions [Helliwell, 1965]. The echo period is 6.8 s.

The hiss in Figure 14 shows strong horizontal striations suggesting their generation or modulation by PLR, as discussed by Park [1977] and Raghuram et al. [1977]. It is not clear what role, if any, PLR played in the triggering of chorus.

August 15, 1974. The spectrograms of Figure 15 illustrate an event that started between 0521 and 0525. Figure 15a shows sudden intensification in the 3- to 4-kHz range starting from the 0525 UT run. As in the August 14 case discussed above, this frequency band does not change noticeably with time. Selected portions of Figure 15a are reproduced in Figures 15b and 15c with expanded scales.

Figure 15b shows that the enhancement in wave intensity at 0525 UT is mostly due to whistlers propagating along a particular duct with a nose frequency of ~3.5 kHz. There are several multicomponent whistler trains such as the one near 20 s, but an examination of expanded spectra before and after 0525 UT shows that the occurrence rate of these long whistler trains did not change significantly. The significant change that did occur at 0525 UT is a sudden increase of the whistler rate on just one path. Near the beginning and end of the record the whistler rate on this path averages about four per second. Note the sharp low-frequency cutoff near 3 kHz. Such an effect is quite common and is due to the limited bandwidth within which whistlers are amplified in the magnetosphere.

In Figure 15c the duct is still active, but the whistlers are more intense than those in Figure 15b, and they trigger emission at the upper cutoff frequency. The lower cutoff has increased to ~3.3 kHz. Triggering is also evident on a few other paths.

Standard whistler analysis [Park, 1980] shows that the active path in Figures 15b and 15c was located at L = 4.6 and had an equatorial electron density of 250 el cm^{-3}. Cyclotron resonance with 3- to 4.5-kHz waves at the equator would require parallel electron energies of 250-900 eV. This active duct was well inside the plasmapause, which was beyond L = 5.1, as evidenced by the lowest nose frequency of the plasmaspheric whistler train such as the one near 20 s in Figure 15b. Thermal plasma density in this duct is not unusually high or low in comparison to that in neighboring ducts, and it is unlikely that energetic particles had a markedly different distribution inside this one particular duct out of many closely spaced ducts. What distinguishes this duct from its neighbors is likely to be its propagation characteristics. We might speculate that this was a superior duct with large density gradients across the wall of the duct or that some irregular structure in the ionosphere increased the wave-coupling efficiency between this duct and the earth-ionosphere waveguide.

In Figure 15d many emissions are seen without any clear sign of triggering waves. However, a detailed examination of the evolution of the wave activity throughout the event reveals a gradual transition in spectra. At first, only whistlers are seen, as in Figure 15b, and then whistler-triggered emissions become evident, as in Figure 15c. Later on, whistlers become weaker, while whistler-triggered emissions become stronger and more numerous until it becomes difficult to identify the whistlers that trigger emissions. Thus we can say with a fair degree of certainty that the emissions in Figure 15d were triggered by whistlers, although the data in Figure 15d alone would not allow such conclusions to be drawn.

A second event of interest on this day occurred near 1200 UT. Figure 16 is a spectrogram for this period showing activity in two frequency bands. The lower band started at ~1150 UT, and the upper cutoff frequency increased from about 0.9 kHz at 1150 UT to about 1.3 kHz at 1215 UT. This behavior is similar to that of the particle-associated events discussed in section 4. Referring to Figure 1, an enhancement in particle flux was observed at 1120 UT following a small substorm that started at 1050 UT. It could be that the VLF activity was related to this flux enhancement.

The upper band, starting at 1210 UT, shows a very different behavior. There is no systematic increase in frequency with time, and strong horizontal striations suggest PLR control. Figure 17 shows portions of the spectra in expanded scales. Multiple lines near 4 kHz show amplitude modulation with approximately 5-s period. By comparing this period with whistler time delays we can establish that PLR was propagating inside the plasmasphere along a duct located at L = 4.3 with equatorial plasma density of 350 el cm^{-3}. For the observed PLR frequency range of 3.5-4.3 kHz the resonant electron parallel energy at the equator is 620-1000 eV. In the 1240 UT run there is a tendency for emissions to come in groups, approximately in phase with PLR. However, since their starting frequencies are not well-defined, we cannot be certain about their association with PLR. The relationship between this event and the particle flux enhancement at 1120 UT is not clear.

August 17, 1974. Figure 18 illustrates the event starting at 1120 UT. Again there is no systematic increase in frequency with time. Three segments of Figure 18a are reproduced in Figures 18b-18d to show spectral details. In Figure 18b we can see that most of the discrete emissions were triggered by whistlers and other emissions. Take, for example, the signals marked A_1-A_9. A_1 is a one-hop whistler with triggered emissions near the upper cutoff frequency. Its low-latitude companion trace, ~1 s earlier, covers the entire 4-kHz bandwidth. The time of the causative spheric in the northern hemisphere is marked by an arrow.

Signals A_3-A_9 appear at the expected arrival times of the successive echoes of signal A_1. However, as before, one can deduce from their spectral shapes that they are not echoes of one wave packet and that new emissions were triggered by echoes of previous emissions. Another ex-

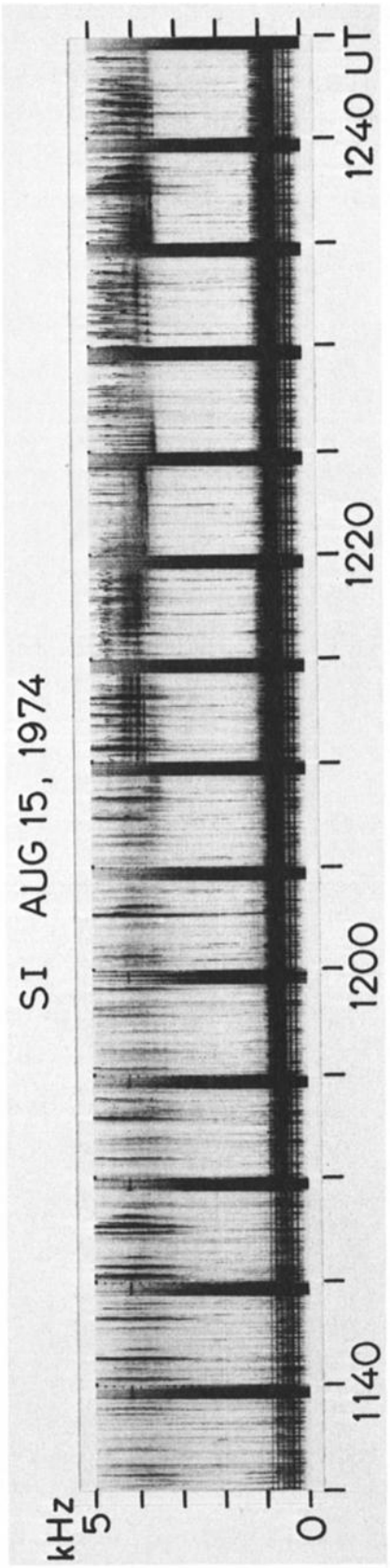

Fig. 16. Spectrograms taken for ~1 min every 5 min.

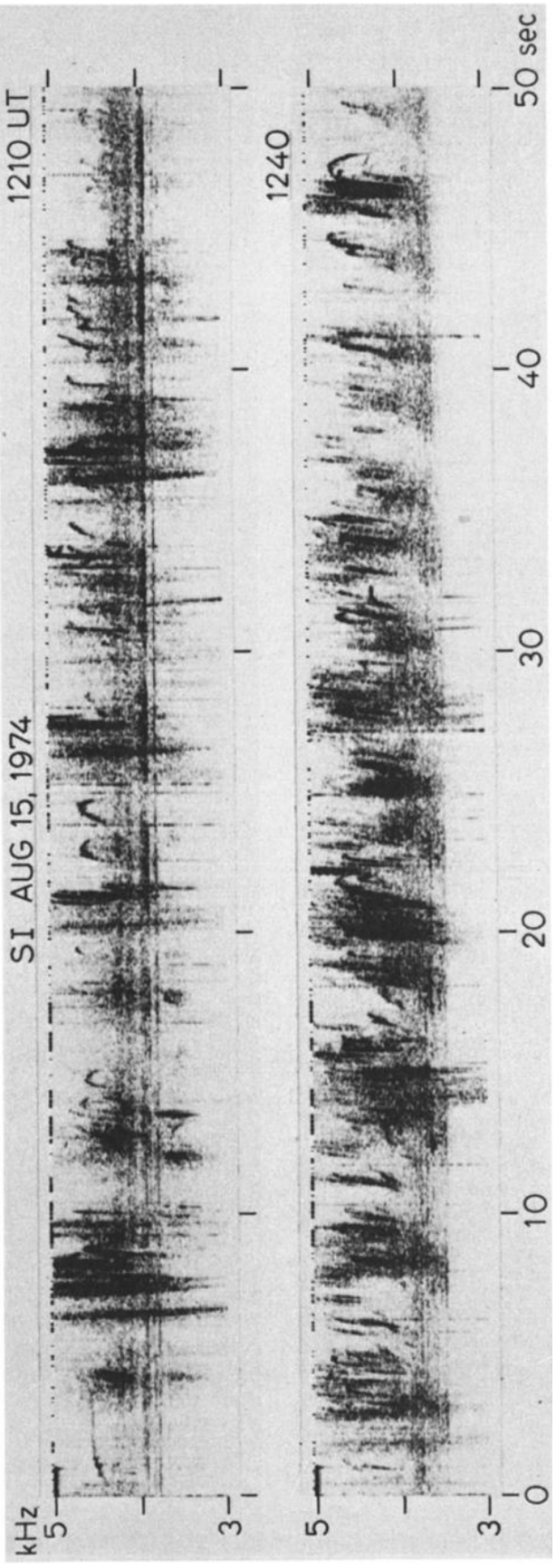

Fig. 17. Expanded spectrograms of two samples from Figure 16.

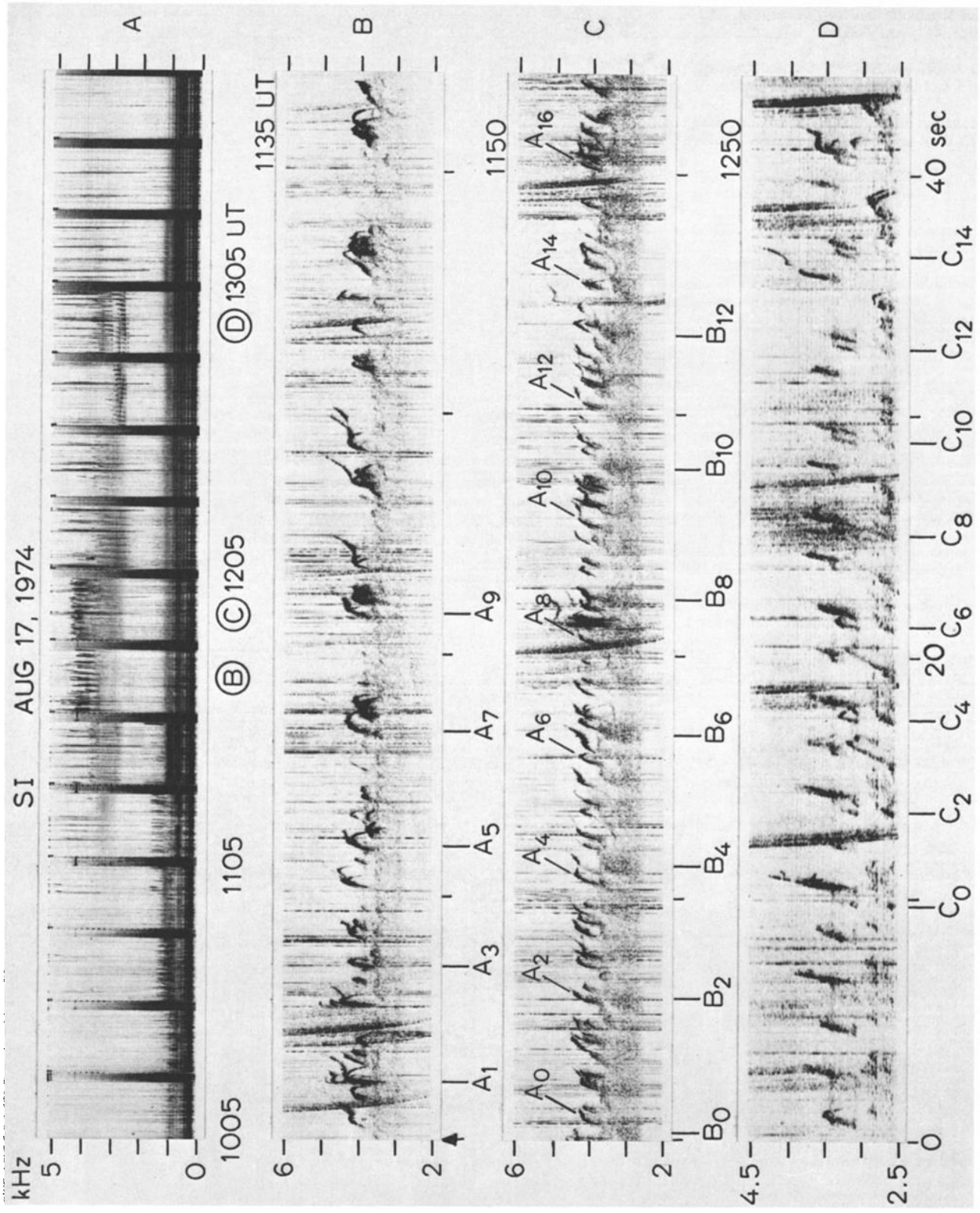

Fig. 18. The top panel shows a series of ~1-min sample spectrograms taken every 15 min. The three lower panels are expanded versions of three samples taken from the top panel.

ample of triggering by echoes can be seen in a series of periodic emissions starting ~0.5 s after signal A_5. Similarly, most of the other emissions in Figure 18b can be traced to echoing trigger signals. An analysis of the whistler A_1 and subsequent emissions shows the duct location at L = 4.5, equatorial plasma density of 220 el cm^{-3}, and equatorial resonant electron parallel energy of 620 eV for a wave frequency of 4 kHz.

In the 1150 UT run (Figure 18c) emissions are more numerous, and therefore it is more difficult to find triggering signals. However, if we use the periodicity in Figure 18b as a guide, we can find several sets of periodic emissions with the same period. One such set is signals A_0-A_{16}. The repetition of the general pattern of emissions between signals A_0 and A_2 is quite clear in the first half of the record, but the pattern becomes somewhat obscured later on as new sets of emissions appear and old ones fade away. The hiss band (~2.5-3.5 kHz) in Figure 18c also shows a periodic pattern, as indicated by signals B_0-B_{12}. The echo period in this case is 5.5 s, whereas the discrete emissions (the A signals) have 4.85-s period. This difference is too large to be explained by the frequency dependence of travel time in one duct. Thus we conclude that chorus and hiss must have propagated in different ducts.

In Figure 18a the emissions at 1235 and 1250 UT show horizontal striations that are believed to be due to PLR. Figure 18d, which is an expanded version of the 1250 UT run, shows many emissions starting at several well-defined frequencies. The periodic nature of these emissions is also apparent. For example, a pair of rising-tone emissions starting at 2.82 kHz (fortyseventh harmonic of 60 Hz) appear periodically with a 3.84-s period, as indicated by signals C_0-C_{14}. The period is somewhat shorter than the periods associated with the A and B signals in Figure 18c, but its magnitude clearly indicates that the path is inside the plasmapause.

Summary of uncorrelated events. VLF wave events not accompanied by particle injection at the synchronous altitude can be summarized as follows. (1) At the time of the event onset the wave upper cutoff frequency does not increase with time as was found to be the case in the events accompanied by particle injection. (2) Wave generation takes place inside the plasmapause where the required electron parallel energy is only ~0.25-1 keV at the equator. (3) Chorus shows evidence of triggering by whistlers, PLR, and other emissions.

6. Discussion and Concluding Remarks

Statistically, chorus tends to occur more frequently outside the plasmapause than inside [Burtis and Helliwell, 1976; Russell et al., 1969]. However, clear examples of chorus generated inside the plasmapause were shown in section 5. We shall refer to the chorus occurring inside the plasmapause as 'plasmaspheric chorus.'

Plasmaspheric chorus interacts (through cyclotron resonance) with electrons with energies of the order of ~1 keV at the equator, a factor of 10-100 less than the resonant energy just outside the plasmapause. Observed growth rates are typically ~20-200 dB/s inside the plasmapause [Stiles and Helliwell, 1977] but ~200-2000 dB/s outside [Burtis and Helliwell, 1975]. The relatively low growth rate inside the plasmapause makes it easier to identify the growth and triggering process in spectrograms. The existence of a trigger threshold has been clearly demonstrated by controlled experiments using the Siple transmitter [Helliwell et al., 1980b]. Details of how this threshold varies with energetic particle parameters is not yet known, but the threshold would presumably decrease with increasing particle flux, thus making it more difficult to detect triggering waves outside the plasmapause where flux levels could be higher. During large particle injection events, chorus could be generated 'spontaneously' in the sense that it can grow out of any existing background noise.

By contrast, plasmaspheric chorus shows that a strong input wave can initiate chorus when the particle flux is not significantly above the quiescent background level. Why plasmaspheric chorus comes in bursts and why it occurs at certain times is not clear. One possibility is an improvement in ducting and echoing properties of one or more ducts that allows strong triggering signals to reach the wave-particle interaction region in the equatorial magnetosphere. One might then think of plasmaspheric chorus as being controlled primarily by propagation conditions, although the trigger threshold may very well depend on energetic particle parameters.

Chorus (or any whistler mode waves) received on the ground must propagate in the ducted mode. This raises a question about how representative ground data are of magnetospheric wave activity. Put in another way, what fraction of magnetospheric wave activity escapes detection at a ground station because of the lack of a duct? We recall that in Figure 1 every major particle injection was accompanied by chorus activity at Siple. Thus it appears that at least during the period of this study there was nearly 100% probability of having a duct within the range of the Siple VLF receiver.

In conclusion, chorus observed at Siple consists of two distinct types. One type of chorus is closely correlated with enhanced electron fluxes with energies of $\gtrsim$5 keV. The upper cutoff frequency increases with time in a characteristic manner at the beginning of chorus events, and the generation region is inferred to be outside the plasmapause. The second type of chorus, which we will call plasmaspheric chorus, is generated inside the plasmapause, is not necessarily accompanied by injection of energetic particles, occurs in band-limited bursts, and does not show systematic increase in the upper cutoff frequency with time. Plasmaspheric chorus shows evidence of being triggered by whistlers, PLR, and echoing emissions. In the case of extraplasmaspheric chorus the role of triggering requires further investigation.

Acknowledgments. We thank J. R. Winckler, C. E. McIlwain, and B. Mauk for providing the ATS 6 particle data for this study; J. Yarbrough, B. Blockley, and T. R. Miller for preparing the illustrations; K. Dean and G. Daniels for preparation of the manuscript; and R. A. Helliwell and D. L. Carpenter for helpful comments. The

research at Stanford University was supported in part by the National Science Foundation, Atmospheric Sciences Section, under grant ATM78-20967 and in part by the National Science Foundation, Division of Polar Programs, under grant DPP76-82646. The research at the University of Washington is supported in part by the National Science Foundation, Atmospheric Sciences Section, under grant ATM77-09080 and in part by the Office of Naval Research under contract N00014-78-C-0333.

The Editor thanks S. D. Shawhan and D. A. Gurnett for their assistance in evaluating this paper.

References

Anderson, R. R., Wave-particle interactions in the evening magnetosphere during geomagnetically disturbed periods, Ph.D. thesis, Dep. of Phys. and Astron., Univ. of Iowa, Iowa City, Dec. 1976.

Anderson, R. R., and K. Maeda, VLF emissions associated with enhanced magnetospheric electrons, J. Geophys. Res., 82, 135, 1977.

Bogott, F. H., and F. S. Mozer, ATS 5 observations of energetic proton injection, J. Geophys. Res., 78, 8113, 1973.

Burtis, W. J., and R. A. Helliwell, Magnetospheric chorus: Amplitude and growth rate, J. Geophys. Res., 80, 3265, 1975.

Burtis, W. J., and R. A. Helliwell, Magnetospheric chorus: Occurrence patterns and normalized frequency, Planet. Space Sci., 24, 1007, 1976.

Carpenter, D. L., Remarks on the ground-based whistler method of studying the magnetospheric thermal plasma, Ann. Geophys., 26, 363, 1970.

Carpenter, D. L., J. C. Foster, T. J. Rosenberg, and L. J. Lanzerotti, A subauroral and midlatitude view of substorm activity, J. Geophys. Res., 80, 4279, 1975.

Cummings, W. D., and P. J. Coleman, Jr., Simultaneous magnetic field variations at the earth's surface and at synchronous, equatorial distance 1, Bay-associated events, Radio Sci., 3, 758, 1968.

Dysthe, K. B., Some studies of triggered whistler emissions, J. Geophys. Res., 76, 6915, 1971.

Foster, J. C., T. J. Rosenberg, and L. J. Lanzerotti, Magnetospheric conditions at the time of enhanced wave-particle interactions near the plasmapause, J. Geophys. Res., 81, 2175, 1976.

Helliwell, R. A., Whistlers and Related Ionospheric Phenomena, Stanford University Press, Stanford, Calif., 1965.

Helliwell, R. A., and T. L. Crystal, A feedback model of cyclotron interaction between whistler mode waves and energetic electrons in the magnetosphere, J. Geophys. Res., 78, 7357, 1973.

Helliwell, R. A., and J. P. Katsufrakis, VLF wave injection into the magnetosphere from Siple Station, Antarctica, J. Geophys. Res., 79, 2511, 1974.

Helliwell, R. A., and J. P. Katsufrakis, Controlled wave-particle interaction experiments, in Upper Atmosphere Research in Antarctica, Antarctic Res. Ser., vol. 29, edited by L. J. Lanzerotti and C. G. Park, pp. 100-129, AGU, Washington, D. C., 1978.

Helliwell, R. A., J. P. Katsufrakis, T. F. Bell, and R. Raghuram, VLF line radiation in the earth's magnetosphere and its association with power system radiation, J. Geophys. Res., 80, 4249, 1975.

Helliwell, R. A., D. L. Carpenter, and T. R. Miller, Power threshold for growth of coherent VLF signals in the magnetosphere, J. Geophys. Res., 85, 3360, 1980b.

Kaye, S. M., C. S. Lin, and G. K. Parks, Adiabatic modulation of equatorial pitch angle anisotropy, J. Geophys. Res., 83, 2675, 1978.

Kennel, C. F., and H. E. Petschek, Limit on stably trapped particle fluxes, J. Geophys. Res., 71, 1, 1966.

Lezniak, T. W., and J. R. Winckler, Experimental study of magnetospheric motions and the acceleration of energetic electrons during substorms, J. Geophys. Res., 75, 7075, 1970.

Lin, C. S., and C. K. Parks, Further discussion of the cyclotron instability, J. Geophys. Res., 79, 2894, 1974.

Mauk, B., and C. E. McIlwain, ATS-6 UCSD auroral particles experiment, IEEE Trans. Aerosp. Electron. Syst., 11, 1125, 1975.

Muzzio, J. C. R., and J. J. Angerami, Ogo 4 observations of extremely low frequency hiss, J. Geophys. Res., 77, 1157, 1972.

Nunn, D., A self-consistent theory of triggered VLF emissions, Planet. Space Sci., 22, 349, 1974.

Park, C. G., VLF wave activity during a magnetic storm: A case study of the role of power line radiation, J. Geophys. Res., 82, 3251, 1977.

Park, C. G., Whistlers, in Handbook of Atmospherics, edited by H. Volland, CRC Press, Boca Raton, Fla., in press, 1980.

Park, C. G., and T. R. Miller, Sunday decreases in magnetospheric VLF wave activity, J. Geophys. Res., 84, 943, 1979.

Park, C. G., D. L. Carpenter, and D. B. Wiggin, Electron density in the plasmasphere: Whistler data on solar cycle, annual, and diurnal variations, J. Geophys. Res., 83, 3137, 1978.

Parks, G. K., Acceleration and precipitation of van Allen electrons during magnetospheric substorms, in Intercorrelated Satellite Observations Related to Solar Events, edited by V. Manno and D. E. Page, pp. 351-363, D. Riedel, Hingham, Mass., 1970.

Parks, C. K., C. S. Lin, B. Mauk, S. DeForest, and C. E. McIlwain, Characteristics of magnetospheric particle injection deduced from events observed on August 18, 1974, J. Geophys. Res., 82, 5208, 1977.

Raghuram, R., T. F. Bell, R. A. Helliwell, and J. P. Katsufrakis, Quiet band produced by VLF transmitter signals in the magnetosphere, Geophys. Res. Lett., 4, 199, 1977.

Russell, C. T., R. E. Holzer, and E. J. Smith, Ogo 3 observations of ELF noise in the magnetosphere, 1, Spatial extent and frequency of occurrence, J. Geophys. Res., 74, 755, 1969.

Stiles, G. S., and R. A. Helliwell, Stimulated growth of coherent VLF waves in the magnetosphere, J. Geophys. Res., 82, 523, 1977.

Storey, L. R. O., An investigation of whistling atmospherics, Philos. Trans. R. Soc. London, Ser. A, 246, 113-141, 1953.

Thomas, T. W., Substorm-related VLF chorus events: Local time dependence and relationship to newly-injected clouds of drifting energetic electrons, Ph.D. thesis, Radiophys. Lab., Thayer Sch. of

Eng., Dartmouth Coll., Hanover, N. H., June 1979.
Thorne, R. M., E. J. Smith, R. K. Burton, and R. E. Holzer, Plasmaspheric hiss, J. Geophys. Res., 78, 1581, 1973.
Thorne, R. M., S. R. Church, W. J. Malloy, and B. T. Tsurutani, The local time variation of ELF emissions during periods of substorm activity, J. Geophys. Res., 82, 1585, 1977.
Tsurutani, B. T., and E. J. Smith, Post-midnight chorus: A substorm phenomenon, J. Geophys. Res., 79, 118, 1974.
Tsurutani, B. T., E. J. Smith, H. I. West, Jr., and R. M. Buck, Chorus, energetic electrons and magnetospheric substorms, in Wave Instabilities in Space Plasmas, edited by P. J. Palmadesso and K. Papadopoulos, p. 55, D. Reidel, Hingham, Mass., 1979.
Walker, R. J., K. N. Erickson, R. L. Swanson, and J. R. Winckler, ATS-6 synchronous orbit trapped radiation studies with an electron-proton spectrometer, IEEE Trans. Aerosp. Electron. Syst., 11, 1131, 1975.

(Received September 13, 1979;
revised May 7, 1980;
accepted June 3, 1980.)